AN ABSTRACT OF THE THESIS OF

Daniel S. Axness for the degree of Master of Science in Bioresource Engineering presented on July 29, 1991.

Title: Estimating Ground Cover via Spectral Data

Redacted for Privacy

Abstract approved:

Marshall J. English

Potato ground cover and spectral data were measured in the Columbia Basin during the 1990 growing season. Three spectral were correlated with ground cover; normalized difference, near infrared-red ratio, and the first derivative of the spectral curve at 750 nm. All models were statistically significant at the 99% level. Normalized was most correlated followed by the near infrared-red ratio, and the first derivative of the spectral curve at 750 nm.

Estimating Ground Cover via Spectral Data

by

Dan Axness

A THESIS

submitted to

Oregon State University

in partial fulfillment of
the requirements for the
degree of

Master of Science

Completed July 29, 1991

Commencement June 1992

APPROVED:

Redacted for Privacy

Professor of Bioresource Engineering in charge of major

Redacted for Privacy

Head of department of Bioresource Engineering

Redacted for Privacy

Dean of Graduate School

Date Thesis is Presented July 29, 1991

Typed by Researcher for Daniel S. Axness

ACKNOWLEDGEMENTS

I would like to acknowledge everyone who has helped me. This is not possible due to the amount of help I have received. Therefore, I will thank a few people and extend my thanks to anyone who has helped.

Susan, my wife, has been very supportive and helpful throughout this experience. Thank you.

My family supported me throughout my entire schooling endeavor. Thank you.

My major professor Marshall English has provided me with many hours of guidance and editing. Thank you.

Chaur-Fong Chen, thank you for being a great workmate and mentor.

Bob Schnekenburger, thanks for the moral support and pizza.

Thank you to the entire Bioresource staff for all the contributions you have made.

NASA provided the funding for this project and my salary, thank you tax-payers. Eastern Oregon Farms, and AgriNorthwest were very helpful in allowing this project access to their land. Thank you.

Table of Contents

List of Figures

List of Tables

Estimating Ground Cover via Spectral Data

CHAPTER 1

Introduction

Ground cover (GC) is defined as the fraction of soil covered by vegetation. Estimates of GC are employed in determining crop coefficients for calculation of evapotranspiration (ET) (Wright, 1982; Cuenca, 1989). Normally ground cover is estimated subjectively by a person in the field, often with just a glance and a guess. Determining ground cover by remote sensing may allow more frequent, consistent measurements than are possible with subjective techniques. Remote sensing allows for whole field ground cover estimation, whereas ground based measurements of GC are limited as to the number and position of sampling locations. Another advantage of remote sensing is the many different scales available. Traditional visual estimation of ground cover has a limited range of scales. In order to approximate ground cover visually, the leaves must be distinguishable from other components on the ground. Some factors that influence the ability to differentiate leaves using photographic methods are: the size of the leaves, the smallest grain size of the photographic film, and the focusing ability of the camera. Spectral remote sensing, is not limited by these factors as components of each pixel are averaged. Thus, there is no need to distinguish individual leaves.

The purpose of the present research was to determine whether remote sensing based on visual and near-infrared spectral reflectance measurements could be used to estimate ground cover with the same or less variation than visual observation methods. In this case, electromagnetic radiation was being sensed, specifically visible and near-infrared light.

Other research at Oregon State University has determined the specific relationship between ground cover and canopy development, and has studied the reflectance of arrays of leaves under laboratory conditions. Using the results from these other studies, it is possible to define the theoretical nature of the relationship between ground cover and reflectance. The present research is an empirical study of that relationship under field conditions.

Spectral reflectance of the plants was defined in this study as the ratio of incoming and outgoing radiation. Incoming solar radiation was measured from the reflectance of a reference panel. Reflected radiation from the plants and soil was measured immediately after the reference panel measurement was taken. The ratio of these two measurements is defined as percent reflectance.

Much research has been devoted to monitoring crop development with different spectral indices based on the reflectances of different light frequencies. For example one such index, red ratio, is defined as the ratio of the reflectance of near infrared light to the reflectance of visible red light. The present research involved first measuring visible and near-infrared reflectances and ground cover of potato canopies throughout the growing season, then deriving empirical models relating ground cover to various spectral indices.

Acquiring spectral data remotely may be accomplished on foot or from a truck, airplane, helicopter or satellite. Scheduling and scale problems ruled out satellites as the data collection platform for the present research, although the results of this research provide useful insights into the potential for use of satellite data. To obtain measurements in a timely fashion it was determined that a mobile, ground based remote sensing platform was needed. The platform chosen was an extendable boom mounted to the bed of a truck. The boom and truck were available at all times and were cost effective compared to helicopters and airplanes.

Measurements of canopy reflectance were taken throughout the growing season in six potato fields in the central Columbia basin. Ground cover (GC) was measured in the field by placing a reference grid over the area of interest and taking a vertical photograph. The photographs were interpreted visually in the laboratory using a method developed by Kollenkark (1982).

The remotely sensed data were used to calculate the values of three spectral indices; Red Ratio (NIR/R), Normalized Difference Vegetation Index (NDVI) and a new index based on the first derivative with respect to wavelength of the reflectance curve at 750 nm. The error in estimating ground cover using these relationships was found to be similar to the variation in the field. Variance observed in the spectral data were of the approximately the same magnitude as the variance of ground cover in the field. Possible sources of variability in reflectance were; moisture on the leaves, different sun angles, diverse soil reflectance, and changes in solar irradiance during measurement.

Ground cover and spectral reflectance were measured throughout the 1990 growing season. Three spectral indices were correlated with ground cover. NDVI was found to be most closely correlated to ground cover, followed by the first derivative of the reflectance curve at 750 nm and Red Ratio. NDVI predicted ground cover well from the time of 20-30 % ground cover until canopy closure occurred.

CHAPTER 2

Literature Review

2.1 Crop Parameters

Spectral estimation of phenological characteristics has been done for many years. Leaf Area Index (LAI) defined by the ratio:

$$\frac{\text{Leaf Area}}{\text{Plant Command Area}}$$

has been the focus of more study than ground cover (Weigand, 1979, Asrar, 1985, Asrar, 1986, Shibayama, 1985, Jordan, 1969, Aase, 1978). LAI provides more information about the state of the plant as it continues to change after canopy closure. However knowledge of ground cover is useful in determining a crop coefficient for purposes of estimating evapotranspiration (Wright, 1982).

Evapotranspiration is generally estimated by an equation of the form:

$$ETa = ETr \times Kc(\tau)$$

Where ET_r is a calculated value of ET for a reference crop (alfalfa or grass) and $Kc(\tau)$ is a crop specific coefficient. $Kc(\tau)$ Is represented as a function of some time scale which corresponds to the phenologic development of the crop. The crop coefficient can be estimated for four growth periods. Those periods are:

(i) Initial period; planting to 10% ground cover (GC).

(ii) Crop development period; from 10% to 70-80% GC.

(iii) Mid-season; from end of crop development to beginning of senescence.

(iv) Late Season; from senescence to harvest.

Wright (1982) has tabulated crop coefficients for the first two periods as a function of the fraction of time from planting to full cover. Thus there is an intrinsic link between ground cover and crop coefficients. Wright also mentioned that crop coefficients based on some other index of crop development would be useful.

Crop coefficients are based on the amount of vegetative material transpiring, and the area of soil evaporating moisture. As the soil becomes covered by vegetation it has less influence on total ET (Wright 1982). The crop coefficients were developed as a basal curve based on a dry soil surface. Adjustments to the crop coefficients are made for wet soil conditions. These changes are significant when the vegetative cover is low. The wet soil condition persists five or more days after irrigation or rainfall.

2.2 Spectral Basis

The remote sensing data collected for this project were based on visible and near infrared light. The colors associated with different wavelengths are presented below in Table 1. Also presented in Table 1 are the wavelengths of sensors on satellite platforms, commonly used for crop monitoring.

Table 1 Wavelengths of Different Colors (μm)				
Wavelength	.4-.5	.5-.6	.6-.7	.7-1.1
Color	Blue	Green	Red	Near infrared
Wavelengths of Several Sensors (μm)				
Sensors	Band 1	Band 2	Band 3	Band 4
SPOT	.50-.59	.61-.68	.79-.89	-
Landsat MSS	.5-.6	.6-.7	.7-.8	.8-1.1
Landsat TM	.45-.52	.52-.6	.63-.69	.76-.9
Spectron SE590	250 bands from 400-1100 nm, bandwidths of approximately 10 nm			

Typical reflectance curves are shown in Figure 1 for soil, healthy potato plants and dying potato plants. These curves illustrate the difference in reflectance characteristics of the different samples. The differences are the basis for vegetation indices.

Curve B illustrates the high near-infrared reflectance typical of healthy vegetation. This high reflectance is probably due to reflectance within the cell wall structure (Mestre, 1935). Another prominent feature is the low reflectance in the red band, due to chlorophyll absorption (Knipling, 1970). Relatively high, green reflectance is evidence of the green visual color. Reflectance of a senescent plant is portrayed by curve C. Overall visible reflectance is higher than that of curve A, however near-infrared reflectance (NIR) is much lower. Soil reflectance is depicted in curve A. Reflectance of soil is typically higher than green vegetation and lower than dead vegetation in the visible region (Tappan, 1980).

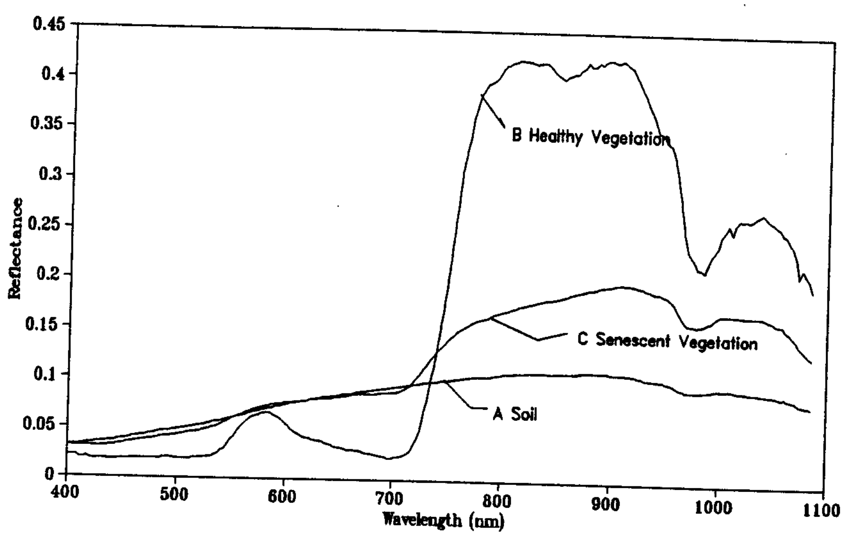

Figure 1 Spectra of Different Field Conditions. Spectral Data from SE590 in 1990

2.3 Research Based on Vegetation Indices

Vegetation indices are based on observed reflectance patterns of vegetation (Perry Jr. 1984). Most indices are based on linear combinations of reflectance bands. Jordan (1969) developed a ratio of near-infrared (.8 µm) to red light (.675 µm), referred to as red ratio or NIR/R, to estimate LAI of a forest canopy. Jordan measured transmitted light at the forest floor and correlated it with LAI. Rouse et al. (1973) developed a relation they referred to as the normalized difference vegetation index (ND). They found that the difference of Landsat MSS bands 7 and 5 (Bands 4 and 2 in Table 1, NIR and Green) normalized by the sum of those two bands had less error in predicting relative greenness. The equation has the form:

$$ND = \frac{NIR - R}{NIR + R}$$

Another normalized difference index that has been found to work well is ND6, the same ratio as ND except that MSS 6 (Band 3 in Table 1) replaces MSS 7 (Perry and Lautenschlager, 1984). Other indices have been developed to improve the predictive powers of spectral data. The Transformed Vegetation Index (TVI) was introduced to reduce the effects of increasing variance with increasing measured values by taking the square root of ND, That is:

$$TVI = \sqrt{\frac{NIR - R}{NIR + R} + .5}$$

The reason for the addition of .5 to the numerator and denominator was to eliminate negative numbers inside the square root. The addition of .5 did not solve the problem. Perry and Lautenschlager (1984) suggest using the formula:

$$TVI6 = \frac{ND6 + .5 \times \sqrt{ABS(ND6 + .5)}}{ABS(ND6 + .5)}$$

This formula is shown to be equivalent to NIR/R for decision making by Perry and Lautenschlager (1984).

Kauth and Thomas (1976) applied sequential orthogonalization to produce an orthogonal transformation of the original Landsat data space to a new four dimensional space. They called it the "Tasseled Cap" transformation, due to the shape of plotted data points. The names attached to the four axes indicate the characteristics to be measured; are as follows: soil brightness index, greenness, yellow stuff, and nonsuch index. The different axes are formed from linear combinations of the 4 MSS bands, as described by Perry and Lautenschlager et al. (1984). The coefficients for each index are derived from site specific soil reflectance information. The transformations allow specific qualities to be estimated from the value of one axis.

Hatfield et al. (1984) used both the Kauth and Thomas index of greenness, and normalized difference with bands similar to MSS 5 and 7 to estimate absorbed photosynthetically active radiation (APAR) with wheat. APAR is directly related to vegetative ground cover (Millard, 1990). APAR decreased due to senescence as greenness decreased. Linear models were chosen to relate both greenness and ND to APAR. The ND index was more correlated to APAR than greenness. Greenness is based on derived coefficients as described above. The ND does not need any derived coefficients (Hatfield, 1984), thus it may be applied without any prior spectral data for the location. This characteristic may make the results from studies using ND more transferrable to other study areas.

Solar angle, irrigation, cultivation and other crop management practices in wheat cultivation have been found to influence spectral estimates of LAI (Asrar et al, 1985a). Reflectance in the red and near infrared bands were used to estimate LAI. A regression model based on previous measurements and a canopy structure model were used to estimate LAI. The estimates from the structure model were generally more correlated than those approximated with the regression technique alone. Irrigation timing and amount affected the plant growth, thus plots with reduced soil moisture were not adequately represented by the regression techniques because of the different growth patterns. The structure based model predicted LAI much better in the water stressed situation than did the regression technique. Row orientation was not found to significantly affect LAI estimates with either method. The regression model and the canopy structure model both underestimated LAI at solar noon. Solar angle was shown to have an effect on estimation of LAI, however other variabilities including intrafield differences and management practices were more significant (Asrar, 1985a).

Much research has been done with remote sensing of wheat and grass based reflectances. Pearson et al. (1976) estimated biomass of shortgrass using a two-band handheld spectral radiometer. The bands selected were 675 ± 25 nm and 800 ±25 nm (roughly red and near infrared). The system developed was able to estimate biomass with a correlation coefficient of .98 for 25 samples. A linear function of the ratio of the two bands was selected. The system worked well for LAI less than 2. Other grassland types with higher LAI were thought to need a non-linear function.

Asrar et al. (1985b) developed a method by which spectral radiation could be used to estimate above ground biomass. The method was based on physical and physiological principles. A 4 band radiometer was used. The bands were similar to those of the multispectral scanner (MSS) on board Landsat satellites. Two algorithms were used to estimate biomass, a simple normalized difference method (similar to ND used in this thesis), and a method based on reflectance modified by crop height, solar angle and crop stress information. Crop stress was measured by thermal infrared temperature readings. The crop stress index was based on the ratio of actual to potential ET (Jackson, 1982). The measurement of the canopy temperature was used to determine the temperature gradient between the canopy and the air temperature. The use of the crop temperature readings significantly improved the estimation of biomass.

Millard (1990) developed significant relationships between cumulative NIR/R and biomass after canopy closure for potatoes. The relationships tended to overestimate biomass at partial ground cover. The crop was neither nitrogen nor water stressed. NIR/R values increased linearly with ground cover after 20% ground cover. (Before that level of ground cover no significant relationship was found.) After full cover, the sum of NIR/R was correlated well with biomass. The researchers felt more work was needed to estimate partial ground covers well.

2.4 Techniques of Field Remote Sensing

The reflectance of a target must be measured at all possible source/sensor positions to completely characterize the target's reflectance domain (Milton, 1987), (Bi-directional Reflectance Distribution Function BRDF). However it is not possible to achieve this in the field. An alternative is standardization of reflected radiance by the use of a reflectance reference panel. The term given to reflectance measured in this fashion is bi-directional reflectance factor (BRF), an alternative to BRDF. To meet the assumptions implicit in using BRF to represent the reflectance of a natural target, the following requirements must be met (Milton, 1987):

(i) The FOV of the sensor is less than approximately 20°

(ii) The reference panel must fill the field of view of the sensor.

(iii) There should be no change in the irradiation amount or distribution between measurement of target and reference panel.

(iv) Direct solar flux dominates the irradiation field; no diffuse sky light.

(v) The sensor responds linearly to changes in radiation flux.

(vi) The reflectance properties of the reference panel are known and invariant over the time of measurements.

Due to ever present sky light the assumption of no background sky light is always violated (Milton, 1987). The other premises may be met through careful preparation and techniques.

Spectral reflectance errors may be caused by nearby objects. Such objects may be people, vehicles, or buildings which may block incoming diffuse light or may reflect more light into the field of view of the instrument. Under certain conditions the errors may cancel. If an object is in the same position with respect to the sample and the reference panel, the contributed reflectance is the same for both measurements. In the field this practice is not always possible. Kimes (1983) chose to model the significance of the error. One example by Kimes included the following assumptions, a 3m X 3m white object 3 m from the target, the reflectance of the white object was .85. This configuration generated less than 2% error in the predicted reflectance.

As discussed above, reflectance properties of the reference panel must remain constant to match the assumptions. Field applications create difficulty in maintaining constant reflectance qualities of the reference panel. Schutt et al.. (1981) found that Halon, a brand name of polyterafllouroethylene, was found suitable for field application as a reference panel because it was washable. Barium Sulfate ($BaSO_4$), the typical reference standard material is not washable. A $BaSO_4$ panel was used as a control in the washing/reflectance tests. The reflectances in the four MSS bands were measured over both the $BaSO_4$ panel and a Halon panel. The reflectance at 5 panel angles from horizontal to 50° were measured. The Halon panel was soiled, washed and the reflectance measured again. The change in the ratio of the reflectances was less than 2 percent for all four bands. Some of that change was due to the different time that the measurements were taken.

Spectral errors may be caused by sequential reference panel readings; i.e. reference panel readings that are not taken simultaneously with plant reflectance readings. Duggin and Cunia (1983) have mentioned that sampling sequentially may introduce such errors. The errors derive from differences in atmospheric conditions between the time when the reflectance standard is measured and the time when the target is measured.

CHAPTER 3

Leaf Area, Ground Cover and Reflectance: Parallel studies at OSU

The fundamental objective of this research was to study the relationship between percent ground cover and canopy reflectance. Both ground cover and reflectance are dependent upon total leaf area and the arrangement of the leaves within the canopy. This study utilized three different sources of data to study the following relationships:

a) The relationship between total leaf area and percent ground cover.

b) The reflective characteristics of leaves, arrayed either as individual leaves or as layers of leaves.

c) The relationship between ground cover and crop spectral characteristics.

The sources of the data used to study these relation ships are listed below:

a) This part of the study was based upon phenologic data collected previously by English, et al. (1989);

b) Laboratory data collected by Chen (1991) were used for this purpose;

c) New field data were collected for this part of the study, as described in the following chapter.

The first two sets of data were collected previously or simultaneously with the present research, with varying degrees of involvement by this author, and are reviewed in this chapter to establish the theoretical relationships involved. The third set of data were collected by this author to determine the corresponding relationships under field conditions.

3.1 Phenological Data

English et al (1989) measured phenological characteristics of several hundred potato plants growing in commercial potato fields. The quantities measured included ground cover, leaf area index and leaf dry weight. The plants were randomly chosen at 5 quasi-random locations in each of 16 different field on three different farms over a period of two years in the Central Columbia Basin. Ground cover was determined from photographs of potato plants in situ. A square reference frame the same size as the row spacing (34 inches on each side) was supported over the potato plants, and a camera centered 6 feet above the frame was used to take pictures of the frame overlaid on the canopy. The apparatus is illustrated in Figure 2. The photographs were interpreted visually to determine ground cover according to a procedure proposed by Kollenkark (1982). The algorithm entailed:

(i) Placing a 19X19 line grid over the frame in the photograph

(ii) Aligning the grid with the frame

(iii) Counting grid intersection points over green vegetation along each row

(iv) Entering total grid intersection count for each transect into a computer program.

The program then determined average ground cover based on the grid counts.

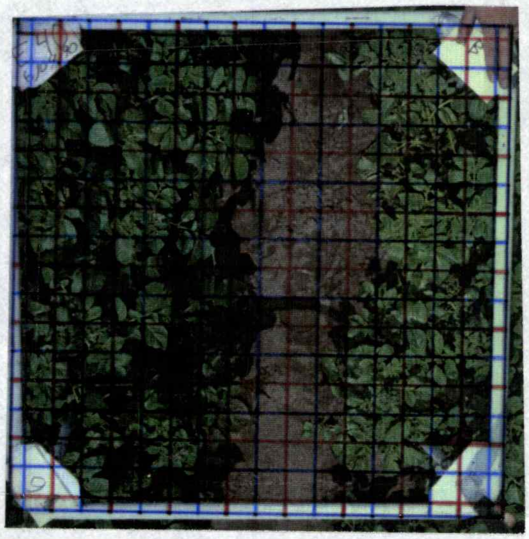

Figure 2 Grid Placed over Potato Plants

Leaf area and leaf dry weight were determined by digging up individual plants and shipping them to Corvallis for processing. The leaves were removed from the plants and optically planimetered. Only green leaves were measured, while dead and senescent leaves were removed from the sample. The leaves were then placed in paper bags and dried at 60°C until no change in mass was detected. The masses and recording methods were verified until confidence was established in the methods. The data were entered in a database which was then authenticated with spot checks of approximately 10 percent of the written records.

Leaf Area Index (LAI) was defined as average leaf area per unit area of ground surface. Phenological measurements obtained in 1988 and 1989 by English and Chen (1989) were used to derive a functional relationship between leaf area index and ground cover. LAI and GC were plotted against each other until canopy closure. Two mathematical models were fit by regression; one linear and the other quadratic. The quadratic model had a slightly better R^2 (.91 compared to .89 for the linear model). By definition LAI and GC must be equal at zero. The linear function does not allow the model to curve to fit the data as well as the quadratic function with this restriction. The quadratic function satisfies the zero intercept requirement and follows the trends of the data better, thus the R^2 was higher. Figure 3 displays the data and the quadratic regression relationship, as well as prediction intervals for a single new observation. The quadratic function derived was:

$$GC=4.9+35\times LAI-3\times LAI^2$$

The prediction intervals were approximately ±14 percent ground cover.

As the quadratic function indicates, GC increases progressively less than LAI as the field approaches full cover. This relationship can be explained by the fact that some parts of the field reach full cover before others. Because the leaf area of the growing plants continues to increase even after canopy closure, the fully covered areas will have an increasing leaf area while GC will remain fixed at 100%. For the field as a whole, the LAI will therefore continue to increase at a steady rate while the rate of increase of GC will decline. Once the canopy is closed, ground cover is not useful for monitoring changes in leaf layers, until senescence begins.

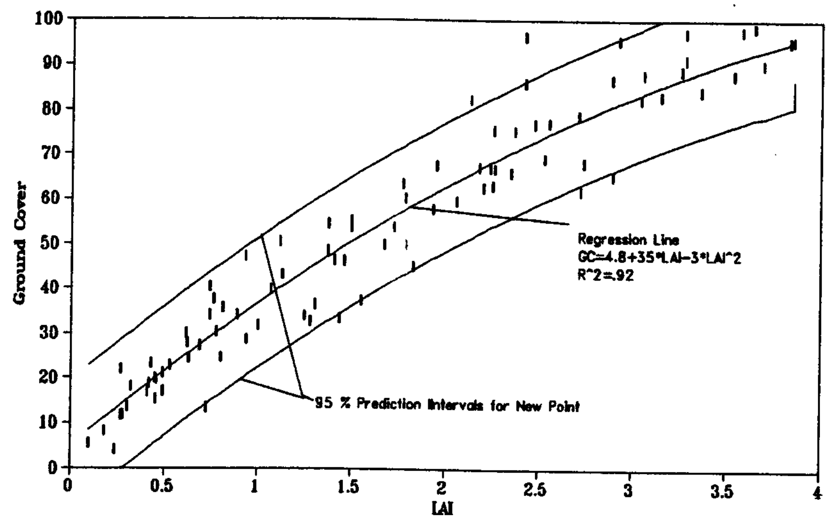

Figure 3 Ground Cover vs Leaf Area Index. Data from 1988 and 1989

3.2 Laboratory Work

Chen (1991) measured the reflectance of St. Johnswort (Hypericum) leaves placed on Eastern Oregon soil. The soil was spread uniformly 1-2 inches deep, and the surface smoothed by hand. The experiment was conducted under 3200K light. The reference panel used was a Halon panel (similar to the panel used in the field as described in the following chapter). During the course of these experiments the field of view was held constant. A Spectron SE590 spectroradiometer was used to collect the spectral data. The SE590 measures intensity of light in each of 250 overlapping bands, spaced approximately 2.6 nm on centers in the range of 400 nm to 1100 nm. The field of view of the sensor used was 15°. The Spectron was recalibrated after the 1990 season by Spectron Engineering (the manufacturer).

Several experiments were conducted to examine the relationship between leaf area and reflectance as well effects of surface slope, moisture and leaf orientation on reflectance.

One set of experiments dealt with near-constant percent ground cover but increasing numbers of leaf layers. This was accomplished by stacking the leaves on top of each other. The stack of leaves covered approximately 7% of the field of view, however the leaves were not perfectly aligned, so slightly more than 7% of the field of view was covered. The spectral curves for different numbers of leaf layers are shown in Figure 4. The NIR reflectance of the stacked leaves increases with each additional leaf, while there is a corresponding decrease in red reflectance.

Another experiment explored the effects of increasing ground cover with a single leaf layer ground cover. The leaves were spread within the field of view and were not stacked on top of each other. Leaves were added one or two at a time to the field of view. The field of view was filled by 12-14 leaves. The spectra from the spread leaves is presented in Figure 5. As more leaves were added, the near-infrared reflectance increased, while the red reflectance decreased.

The data taken by Chen were used to calculate values of NIR/R and ND6 a linear relationship between the amount of soil covered by leaves in a single layer (GC) and NIR/R and ND6. The relationships are illustrated by Figures 6 and 7. Figure 6 compares

NIR/R vs. number of leaves for stacked and spread leaves. Figure 7 plots ND6 against the number of leaves. The spread leaves are represented by the upper line, while stacked are illustrated by the lower line. The shape of the curves for stacked and spread leaves can be explained in terms of a simple model of reflectance.

$$\rho = \rho_{plant} \times GC + \rho_{soil} \times (1 - GC) + \rho_{interaction]}$$

Where:

(i) ρ is total reflectance of sample.

(ii) ρ_{plant} is light reflected before it hits the soil.

(iii) ρ_{soil} is light reflected by soil without passing through any leaf tissue, and

(iv) $\rho_{interaction}$ light which is reflected by the soil but is attenuated by passing through the leaves either before or after reflection from the soil.

The reflectances in this model vary with the band of light being modeled, e.g. Red or NIR. Figure 8 is a drawing of light interaction with leaves. Rays 3 and 5 are examples of ρ_{plant}. Ray 9 is an example of ρ_{soil}. The other rays interact with both the soil and the plant (rays 8 and 11).

In the case of leaves spread in a single layer, the leaves were placed directly on the soil, therefore any reflection from the soil underneath the leaf would necessarily pass through the leaf twice (rays 8, 11). Since leaf transmittance in the red band is low, very little light would pass through the leaf twice. Thus red reflectance through the leaves would contribute little to the measured reflectance. The NIR reflectance of soil is approximately 17%, and the transmittance of the leaf is at most 50%. Consequently, near infrared light that has passed through the leaf, reflected from the soil, and passed through the leaf again will be no more than 4% of the incoming NIR radiation. The sum of radiation represented by rays 3 and 5 is equal to the reflectance measured over the full cover situation. Thus, the amount of light attributed to ray 5 is the difference between the sum and the amount of ray 3. Figure 5 shows the spectra of the spread leaves. The average reflectance in the NIR region (790-1000 nm) at full cover is approximately 46 %. The amount associated with direct leaf reflectance (ray 5) is therefore approximately 42% of the incoming light.

Reflections from bare soil would not intercept any leaves, because the leaves are laid flat on the soil. The linearity of the data is therefore explained by the simple reflectance equation and the geometry of the plant leaves. This concept is important in understanding the relationships between vegetative cover and reflectance.

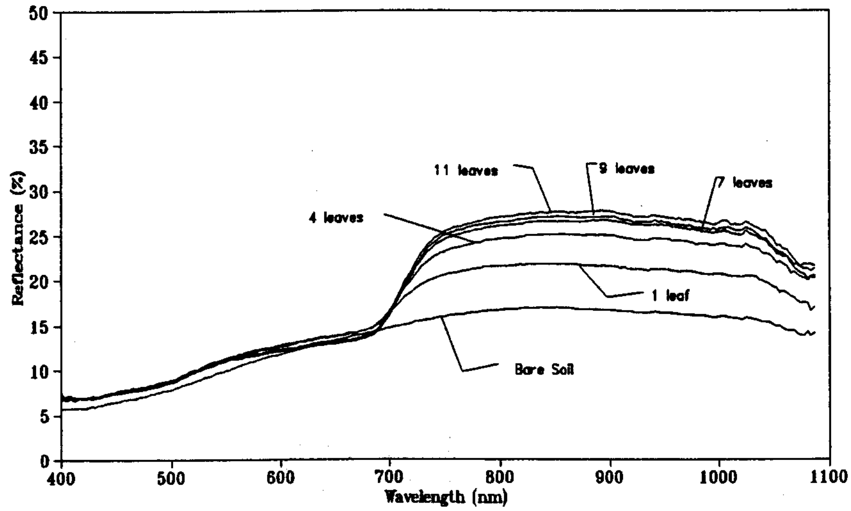

Figure 4 Plant-Soil Response (@3200 K). Leaves Stacked in Field of View.

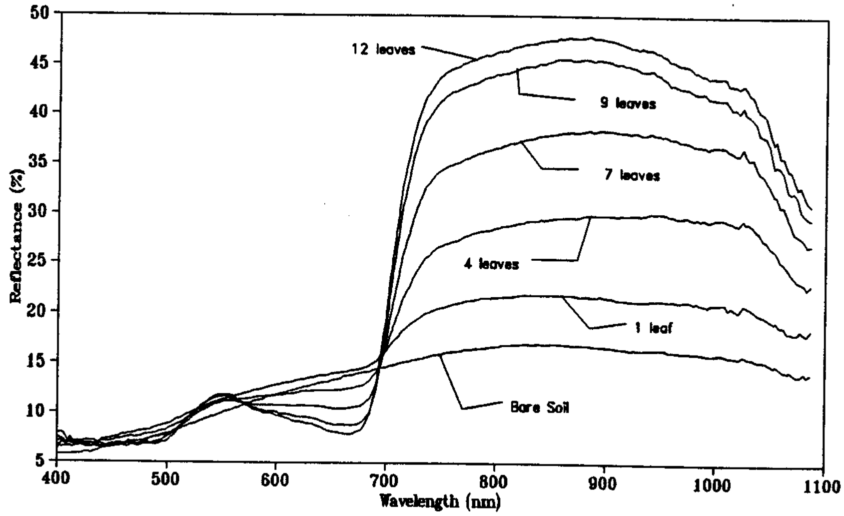

Figure 5 Plant-Soil Response (@3200 K). Leaves Spread in Field of View.

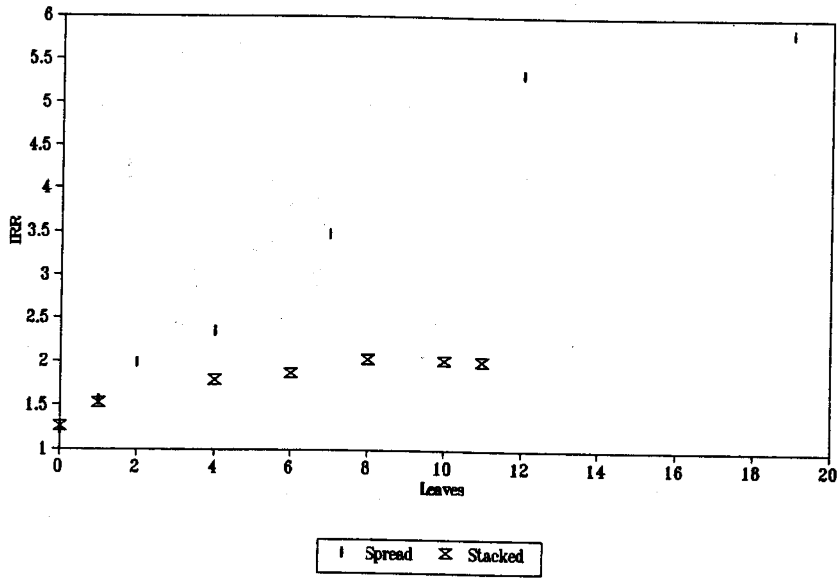

Figure 6 Near Infrared-Red Ratio vs. Number of Leaves. Leaves both Stacked and Spread in Field of View.

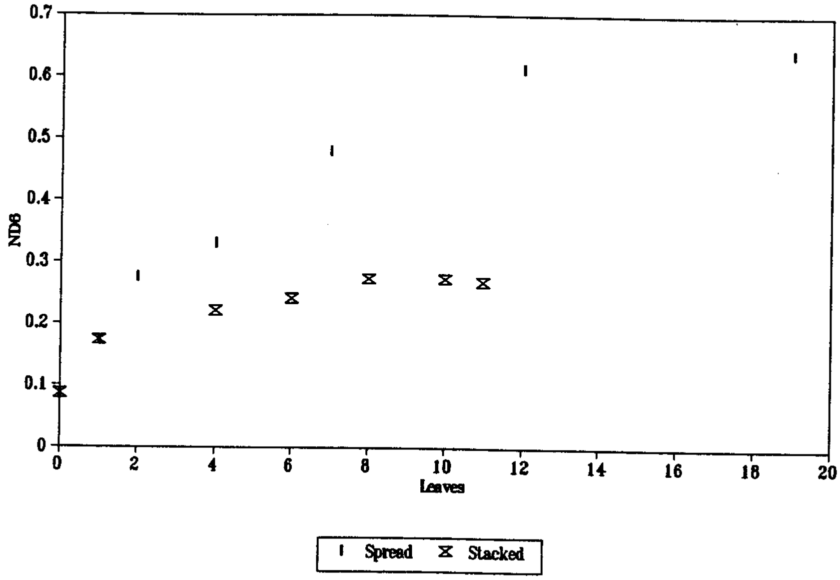

Figure 7 ND6 vs. Number of Leaves. Leaves both Stacked and Spread in Field of View.

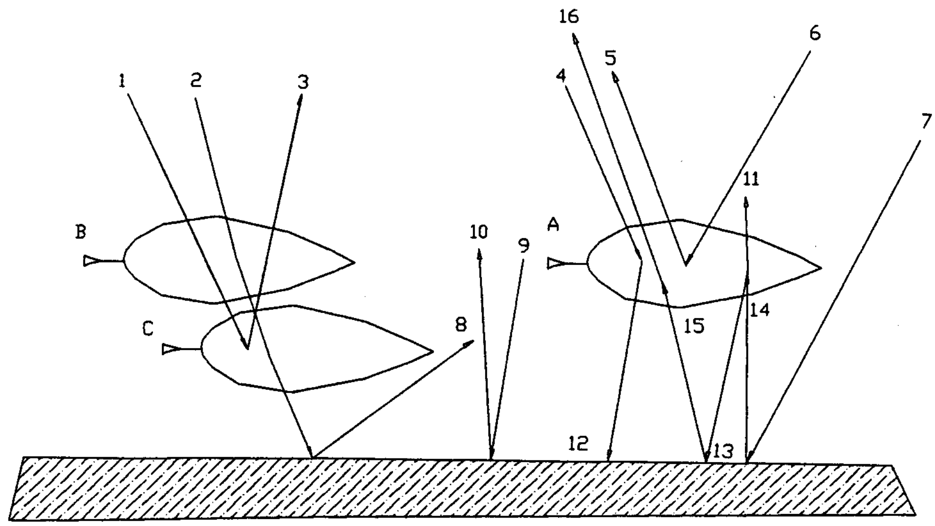

Figure 8 Diagram of Leaf and Light Ray Interaction.

Spectral indices appear to be proportional to single leaf layer GC, based on the data taken with single layer leaves. This linearity depends upon a linear relationship between ground cover and leaf area index. However, multiple leaf layers do continue to form, with nonlinear results suggested by the stacked-leaves data.

The relationship chosen to fit these data was an exponential form, as the spectral indices increased at a decreasing rate. The indices show a decreasing rate of increase in red reflectance as the number of layers increases, probably due to slight misalignment of the leaves. NIR reflectance shows an increase until there are about 8 leaves in the stack. Beyond that point the near-infrared light that penetrates through all 8 layers is very small. The light passes through 7 leaf layers on the path to the eighth leaf. Each layer transmits up to half the incident light. The fraction of light striking the eighth layer is $.5^7$ times the original incident light. Under optimum conditions the eighth layer reflects 50 percent of the incident light. At this point $.5^8$ times the original light is reflected upward. The same process ensues on the path upward. The result is that $.5^{15}$ times the original light is transmitted to the sensor.

The amount of light reflected, transmitted and absorbed in each layer depends upon the light frequency involved. Leaves collectively reflect and transmit up to 90 % of near-infrared light (Knipling 1970), whereas light in the visible band is largely absorbed by the chlorophyll in the plant leaves. Most visible light is absorbed by the first three layers (Knipling, 1970).

Dew or irrigation on vegetation increases variability as shown by Pinter Jr. (1986). Some of the fields sampled during the season had just been irrigated. To examine the effects of irrigation on reflectance, the leaves were progressively wet with water to simulate irrigation or dew. In this case, the leaves filled the field of view as described above. The treatments were subjectively described as ranging from dry to very wet. Irradiance measurements were taken rapidly to limit the changes due to drying of the leaves, and moisture. The changes in reflectance are shown in Figure 9. The same leaves and configuration of leaves was used throughout the experiment, the only variable was the applied moisture. The spectra of the leaves remained the same, except for the variation caused by the moisture. The NIR/R ratio shows much more variation, than the NDVI as indicated by the ratio of standard deviation and the mean; .1 for NIR/R, and .036 for NDVI (Figures 10 and 11). The interaction between leaf canopy and reflectance becomes much more complicated with multiple leaf layers, greater depth between leaf layers, and random leaf angles. This increased complexity was evaluated empirically using reflectance measurements from potato crops under ordinary field conditions, as described in the next chapter of this thesis.

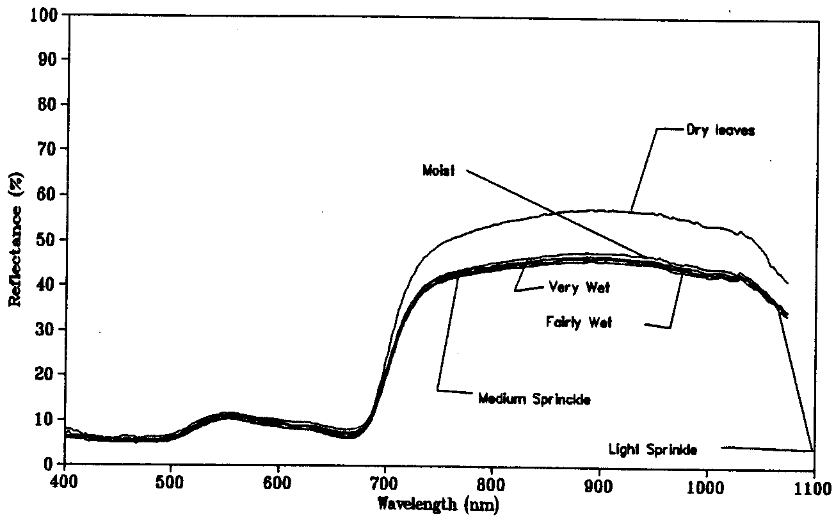

Figure 9 Spectra of Spread and Moistened Leaves. Dry and Moistened Leaves (Chen, 1991).

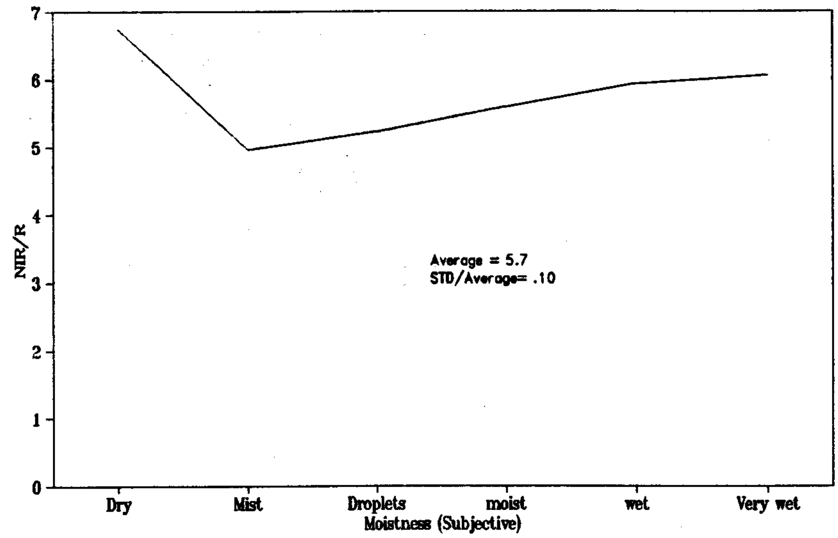

Figure 10 Near Infrared-Red Ratio vs. Subjective Moisture. Spread Leaves in Field of View. (Chen, 1991)

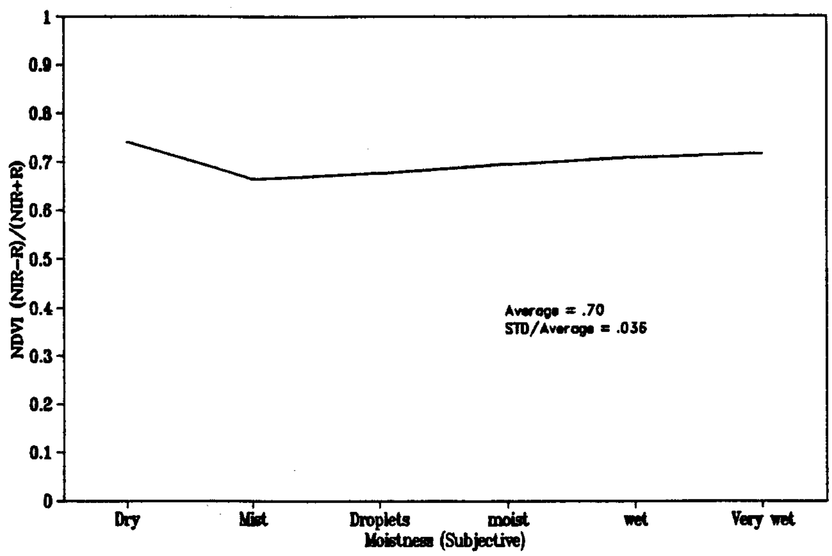

Figure 11 NDVI vs. Subjective Moistness. Spread Leaves in Field of View. (Chen, 1991)

CHAPTER 4

Ground Cover and Reflectance Under Field Conditions

4.1 Field Conditions

The relationship between ground cover and canopy reflectance was studied under field conditions in Eastern Oregon during the 1990 growing season. The study concentrated on potatoes, though other crops were examined as well. Data were taken in 6 fields in Eastern Oregon and Eastern Washington. The fields in Oregon were 5 miles east of Boardman, Oregon. The fields in Washington were 3 miles north-east of Umatilla, Oregon. In each field, 6 representative sites were staked and used throughout the season (Figure 12). The fields near Boardman all had the same soil type, Quincy fine sand, excessively drained with rapid permeability. The fields near Umatilla had several soil types: Field 1, Quincy Loamy sand, excessively drained, rapid permeability with low water holding capacity; Field 47 Quincy loamy sand; Field 58, Warden very fine sandy loam, well drained, moderately permeable with high water holding capacity.

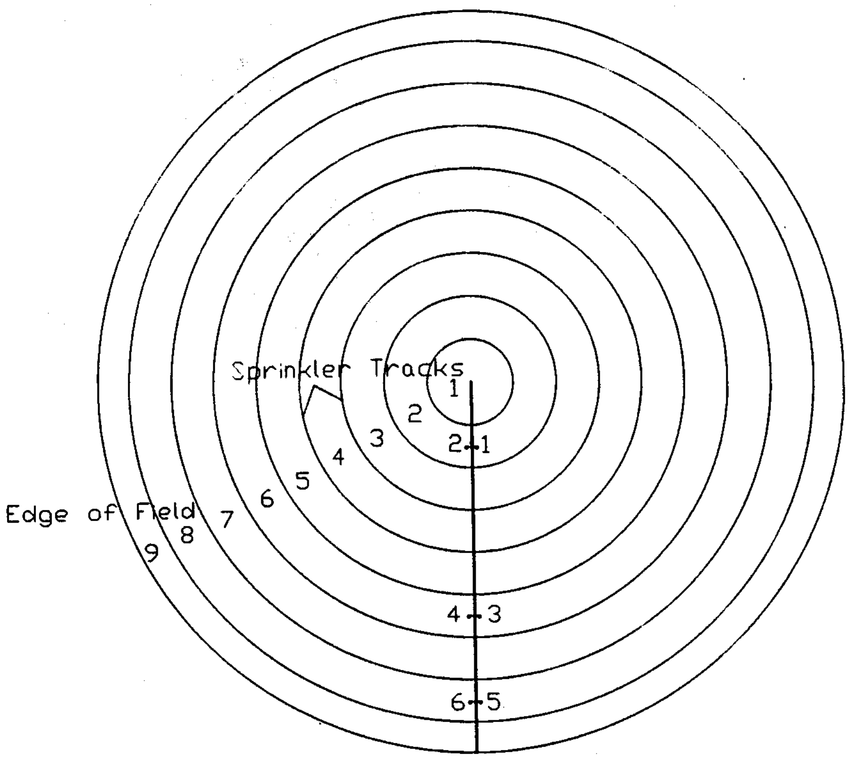

Figure 12 Diagram of Typical Field Samples were Taken From. (English 1988, 1989; Axness 1990).

Ground cover was measured from photographs of a 34 inch square grid overlaid on the canopy as described in Chapter 3. Four samples of ground cover were taken at each spectral sampling point. Four photographs were taken at 90° intervals around the stake, giving four ground cover readings at each sample point. The mean of the four measurements was used as the ground cover for that position.

The same Spectron SE590 spectroradiometer used for studies of reflectance of individual leaves (see section 3.2) was used to collect the field spectral data. The field of view (FOV) used was 15°. The SE590 was attached to the end of a truck mounted boom, and could be positioned from 6 to 30 feet above the soil surface. The measurements were taken at 30 feet above the soil surface for this experiment. The field of view (FOV) at this height covered 49 $feet^2$ (4.6 m^2) and encompassed approximately 2.8 rows. The attachment for the SE590 was self-leveling and held the sensor in a nadir position (Figure 13). A camera loaded with near-infrared panchromatic film was also attached to the boom. This camera was set to have nearly the same FOV as the Spectron.

Since incident solar irradiance is variable, the ratio of reflected light to incident solar light is a more consistent measurement of spectral characteristics than the magnitude of reflected light by itself. The incident irradiance was measured by measuring the reflected light of a 99% reflectance standard (Spectrolon reflectance panel). The reflectance characteristics of the panel were supplied by the manufacturer. Figure 14 shows reference panel readings throughout one day. The variations in these readings are an indication of the variability of incident light and the effects of changing sun angles throughout the day.

Figure 13 Boom Truck in Potato Field.

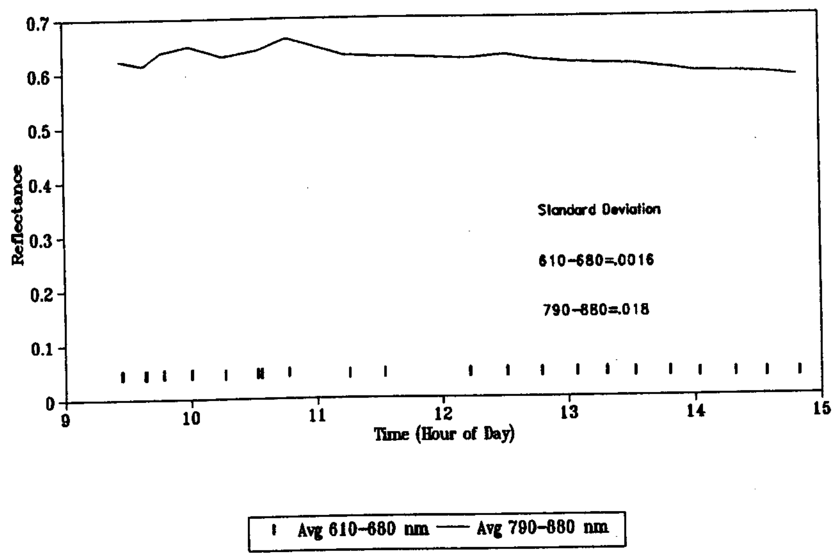

Figure 14 Reflectance vs. Time. Spot Bands 2 and 3 Simulated From SE590, Hermiston 6-20-90

The data were down-loaded from the Spectron to a portable IBM compatible computer. Several programs were written to arrange the data for analysis. The collation of the data was done in a spreadsheet and the data were stored in an ASCII file. Ground cover, date, and time were stored with each record.

Measurements of reflectance were taken from 10 AM to 3 PM Pacific Daylight Savings Time with solar noon occurring at 1:00 PM. A reference panel measurement was taken immediately before or after the spectral data were collected at each of the six sites in each field. GC was estimated at each site as described above.

4.2 Sources of Error

Primary sources of error in field measurement were:

(i) the influence of nearby objects

(ii) variations between reflectance measurements of the target and of the reference panel

(iii) variations caused by the changing reflectance characteristics of the reference panel.

Nearby objects may influence the sensed reflection of a target. Kimes (1983) discusses an example more extreme than this project's situation. The assumptions about nearby objects made by Kimes could be applied to this project. The circumstance examined in Kimes analysis included a 3X3 meter white van 3 meters away from the target. The error predicted for that circumstance was less than 2 percent. The situation for this project was:

(1) the field of view was a 15° viewing cone from 30 feet elevation

(2) the nearby object was a light tan pickup (less reflective than white) which supported the boom.

(3) the target was 12 feet away (more than 3 m)

The error in the actual field situation is therefore assumed to be less than the 2% error predicted above by Kimes.

The reference panel was a very important part of this remote sensing project. All measurements were referenced to it. Maintaining the same reflectance qualities throughout the season was critical. When the panel became soiled through normal use it was washed as described by Schutt (1981).

4.3 Results

4.3.1 Spectral Characteristics and Ground Cover in the Field.

Typical spectral characteristics for potatoes are illustrated by Figure 15 which shows reflectance as a function of wavelength at one position in a field throughout the season. The GC measurements for that location are shown in Table 2. The spectral profile of bare soil is indicated by the lowest curve, identified by Julian Date (JD) 124. At 22% GC (JD 136) there is evidence of crop emergence, indicated by an increase of near-infrared reflectance. Visible wavelength reflectance does not change much at the lower GC and absorbance is not much higher than that of soil.

After GC reaches about 30 percent (after JD 138) the green (500-600 nm) reflectance remains relatively unchanged while reflectance of the other visible wavelengths decreases. However near-infrared reflectance becomes much higher with increasing ground cover. Multiple leaf layers enhance near-infrared reflectance because infrared light that passes through the top layers may be reflected by lower layers. As crop canopies close, up to approximately five leaf layers are formed as indicated by leaf area index.

Measurements from the field are presented in Table 1 in the Appendix. The location refers to the positions in each field indicated in Figure 12, which shows a definition sketch of a typical center pivot field. The values following ground cover in Table 1 of the Appendix are the calculated values of various spectral indices including: normalized difference, NIR/R and slope at 750 nm.

Table 2

Ground Cover; Eastern Oregon Farms

Julian Date	Ground Cover	Weather
124	0	Mild Hazy
136	22	Mild Hazy
141	35	Clear
159	79	Cloudy
165	99	Clear
203	100	Clear

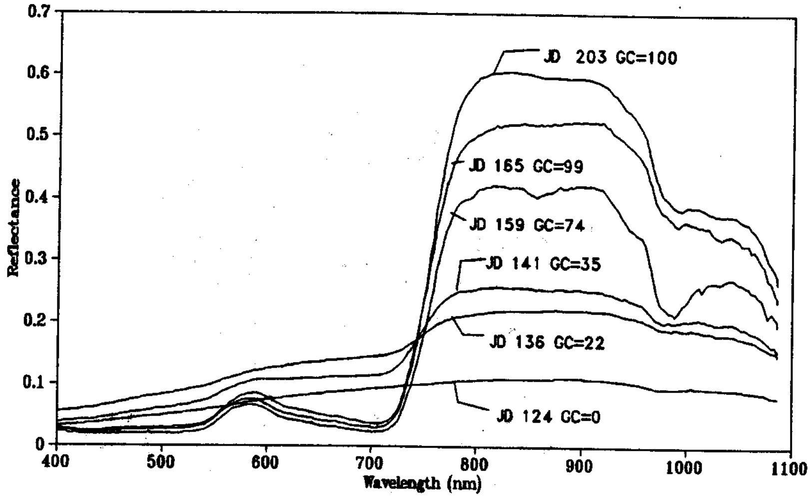

Figure 15 Spectra From Eastern Oregon Farms, Field 40, Position 4. SE590, 1990

4.3.2 Vegetative Indices vs. Ground Cover

As discussed earlier, past research has indicated that ratios of reflectance values in two or more bands can be excellent indicators of canopy development. The specific wavelengths chosen were 700-800 nm (NIR) and 600-700 nm (Red), with the basis for choosing these bands being that they are Landsat bands. Empirical models for estimating ground cover based on NIR/R, ND6 and the first derivative of the reflectance curve were therefore developed using the field data described above. (The calculated values of these indices are summarized in the appendix.) The empirical models were compared to determine which would be most effective for estimating ground cover by remote sensing. In the discussion that follows, the phrase "individual point" refers to each reading at any one of the six locations in each field. The word 'mean' refers to the average of the six readings taken in each field.

The relationship between red ratio and GC appears to be curvilinear. A quadratic function was therefore fit to the data by regression (R^2=.92):

$$\text{Ground Cover} = -34 + 43 \times \frac{NIR}{R} - 3.57 \times \left(\frac{NIR}{R}\right)^2$$

The function is represented in Figure 16. The upper and lower lines represent the 95% prediction intervals for individual points. The prediction interval at 60% ground cover is ±18% ground cover. The inner lines represent 95% confidence interval for the mean of 6 samples at that point. The confidence interval for the mean of 6 samples at 60% GC is ±6.8%.

As can be seen from Figure 16, at low GC, NIR/R does not react to small changes in ground cover. This index may not be suitable for use at low ground cover.

The Normalized Difference ratio is denoted as ND6 and has the form:

$$\frac{NIR-R}{NIR+R}$$

This ratio has been used extensively to monitor vegetation (Tucker, 1979). GC is plotted against ND6 in Figure 17. The regression is given by the following equation (R^2=.94):

$$\text{Ground Cover} = -4.2 + 138.6 \times \frac{\text{NIR}-\text{R}}{\text{NIR}+\text{R}}$$

The prediction interval for any single point is ±17%. The confidence interval for the mean of six samples at 60% ground cover is 2.2%. Unlike NIR/R, ND6 appears to be more sensitive to changes in GC early in the growth period.

Upon observation of spectra collected during the summer of 1990, a third vegetation index was developed; the first derivative of the spectral curve at 750 nm, defined as:

$$\frac{dR_n}{d\lambda} = \frac{R_{750nm} - R_{747nm}}{750\text{nm}-747\text{nm}}$$

where R_n = Reflectance of a 10 nm band centered at a frequency of n nanometers

Ground cover is plotted against this index in Figure

18. The regression equation was (R^2 = .93):

$$\text{Ground Cover} = 1.5 + 13834 \times \frac{dR}{d\lambda} - 481420 \times \frac{dR^2}{d\lambda}$$

The 95 percent prediction and confidence intervals were respectively, 21 and 4 percent ground cover.

The data presented in Figures 16, 17 and 18, represent individual points in the fields; six sites were sampled in each field on each day of data collection.

It is interesting to observe the reduced variability when field averages (the averages of all six points for each field) are plotted against ground cover (Figures 19, 20 and 21). Average GC from each field and each date are plotted against the average NIR/R (Figure 19), average ND6 (Figure 20), and the average first derivative at 750 nm (Figure 21).

These averages from each field may be regarded as approximations of field-wide averages of the indices. The reduced variability may be due to averaging some physical features, such as slope, aspect or soil dampness. Alternatively, since the data were taken at different times over a period of perhaps 45 minutes in each field, the effects of the variation in cloud cover might be masked by these averaged data.

The function fit to the average NIR/R data was:
(R^2=.92)

$$\text{Ground Cover} = -35 + 44 \times \frac{\text{NIR}}{\text{R}} - 3.8 \times \frac{\text{NIR}}{\text{R}}^2$$

The regression function used to fit the average ND6 data was: (R^2=.95)

$$\text{Ground Cover} = -9.2 + 127 \times \text{ND6}$$

The regression function used to fit the average First Derivative data was quadratic in form: (R^2=.94)

$$\text{Ground Cover} = -1.28 + 15094 \times \frac{dR}{d\lambda} - 621400 \times \frac{dR}{d\lambda}^2$$

All of the functions discussed above had significant F-ratios at 99% probability or greater.

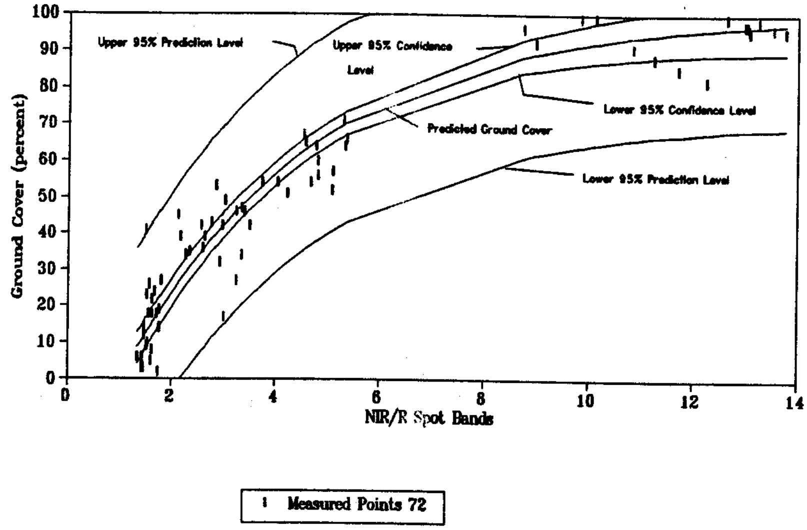

Figure 16 Ground Cover vs. Near Infrared-Red Ratio. Spot Bands Simulated With SE590, 1990

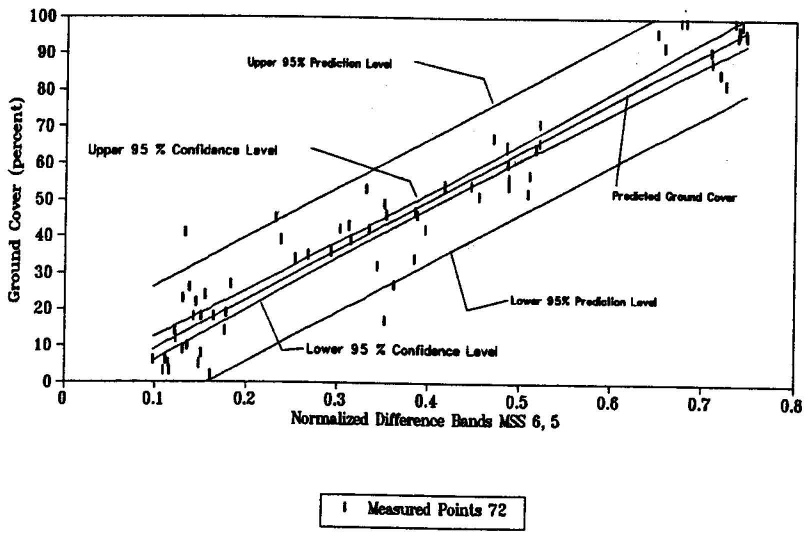

Figure 17 Ground Cover vs. Normalized Difference. Simulated With SE590, 1990

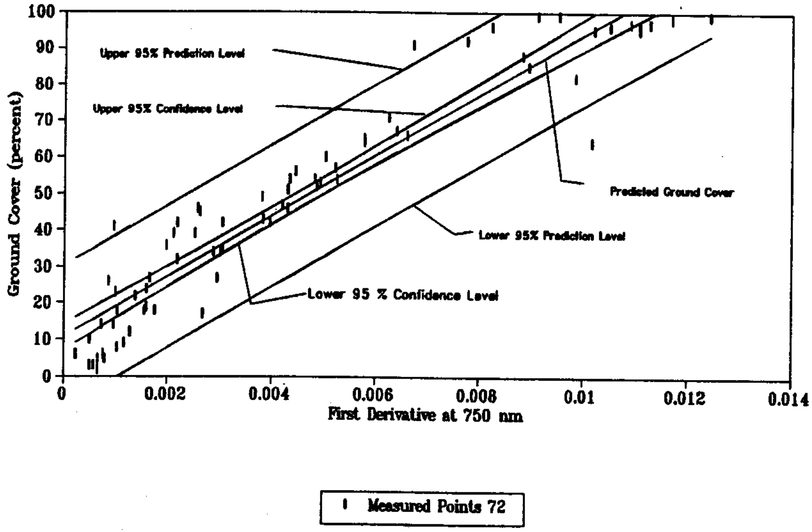

Figure 18 Ground Cover vs. First Derivative at 750 nm. SE590, 1990

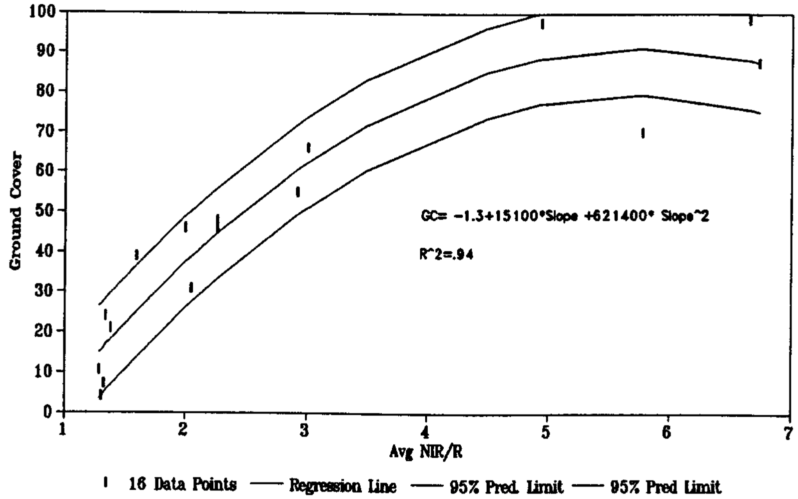

Figure 19 Average Ground Cover vs. Average Near Infrared-Red Ratio

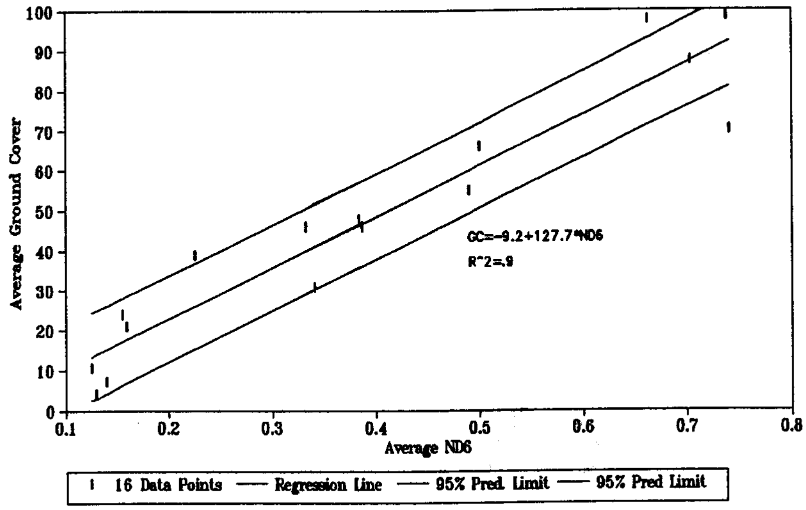

Figure 20 Average Ground Cover vs. Average ND6.

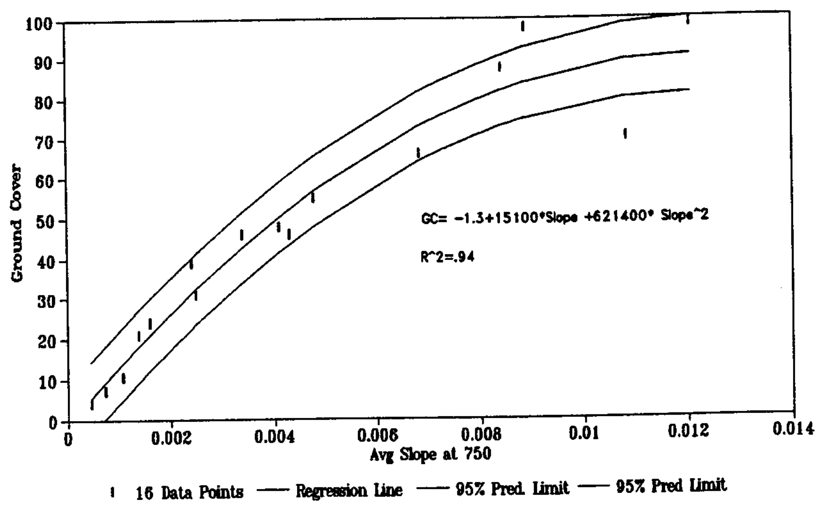

Figure 21 Average Ground Cover vs. Average First Derivative at 750 nm.

4.3.3 Influence of Sun Angle and Viewing Angle

The time of day when measurements are made can noticeably affect reflectance characteristics, primarily because of changes in the sun angle. The influence of time-of-day on the three reflectance indices was examined by taking continuous readings from 9:00 AM to 3:00 PM at a single site in a field with full cover. The effects of sun angle on reflectance in red and near infrared bands are shown in Figures 22 and 23. The standard deviation is 3% of the average for the day for the NIR band. The same statistic is 3.6% for the red band. NIR/R, ND6 and slope at 750 nm were plotted against time of day in Figures 24, 25 and 26. ND6 is less sensitive to time of day than the other two indices.

Different viewing angles can also influence the reflectance in all bands and the ratios between the bands (NIR/R and ND6). This is shown for two fields with full canopy cover, based on reflectance measurements in the morning and in the afternoon, in Figures 27 and 28. The spectra of the sunlit canopy has a greater reflectance as well as a higher red ratio. Three of four nadir-view measurements have greater NIR/R values than shaded canopies.

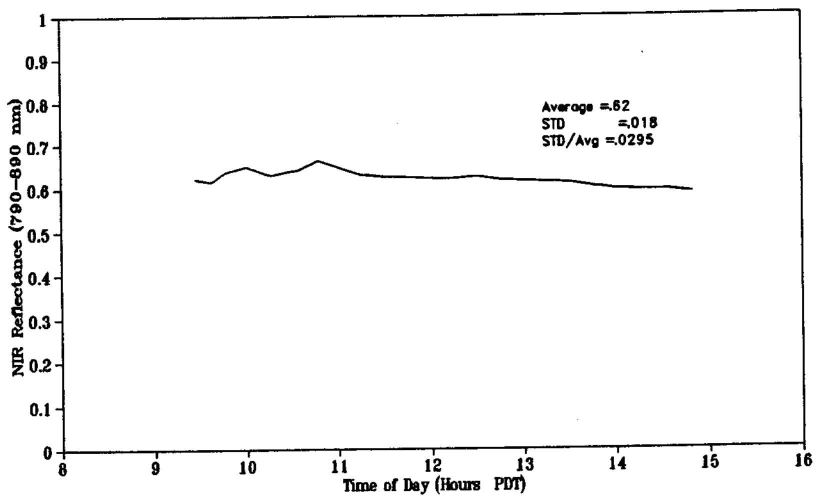

Figure 22 Near Infrared Reflectance vs. Time of Day. EOF 40, 6-20-1990

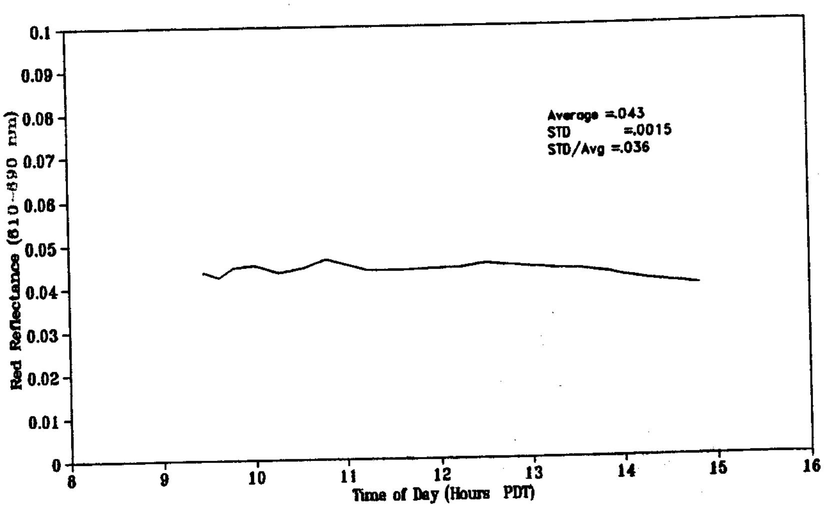

Figure 23 Red Reflectance vs. Time of Day. EOF 40, 6-20-1990

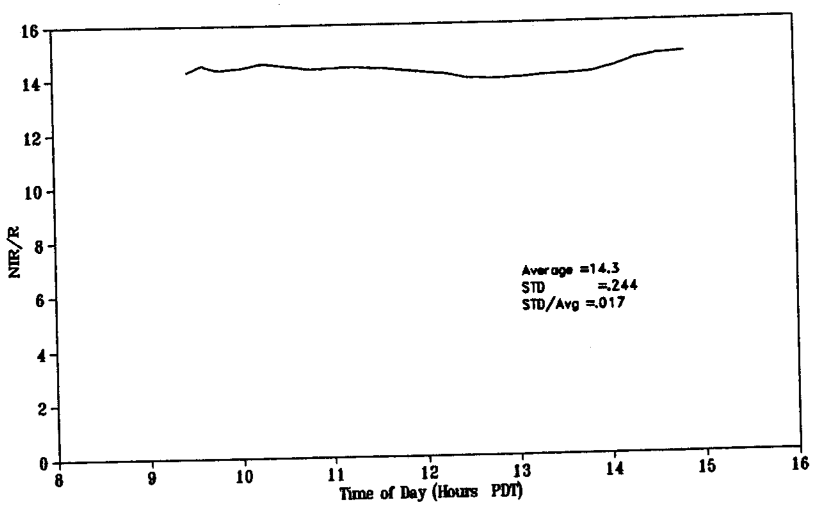

Figure 24 Near Infrared-Red Ratio vs. Time of Day.
EOF 40, 6-20-1990

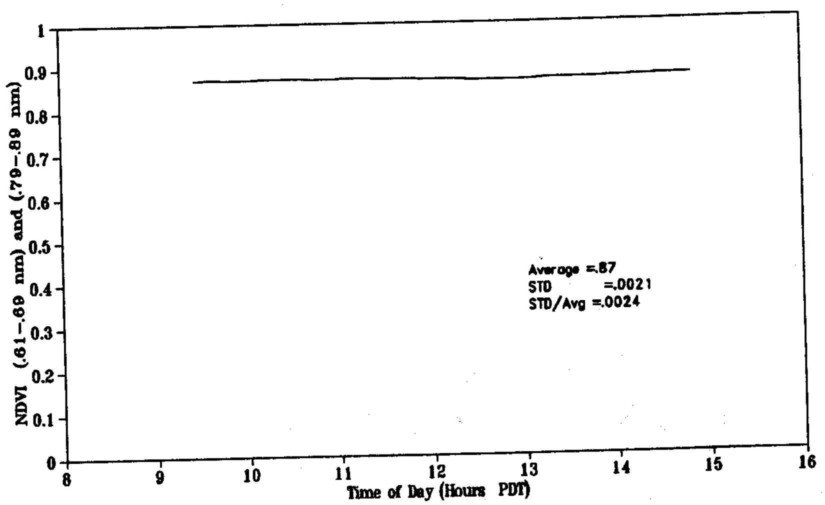

Figure 25 ND6 vs. Time of Day. EOF 40, 6-20-1990

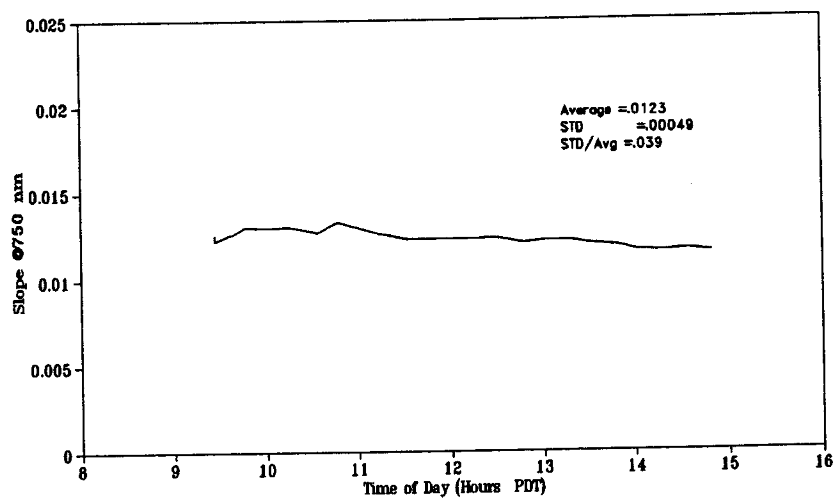

Figure 26 First Derivative at 750 nm vs. Time of Day. EOF 40, 6-20-1990

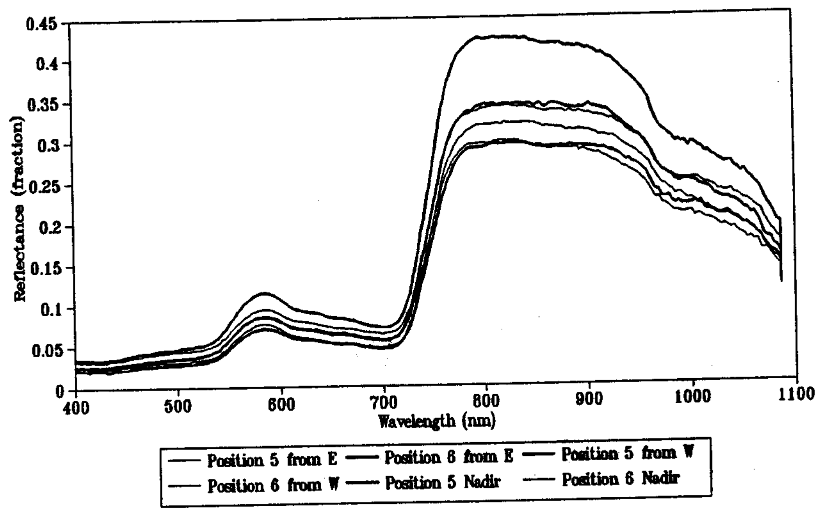

Figure 27 Off-nadir Viewing -McNary 47. 15 Degrees off from East and west at 13:50 PDT

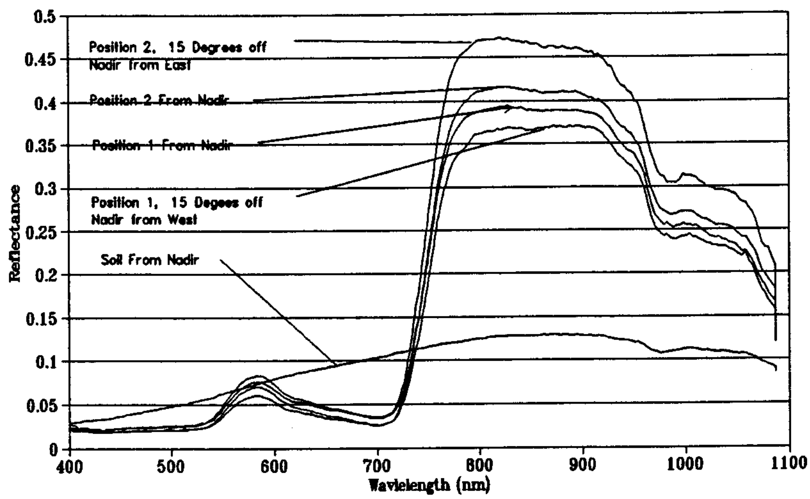

Figure 28 Off-nadir Viewing -EOF 40. 15 Degrees off from East and west. At 11:00 PDT

CHAPTER 5

Conclusions

5.1 Empirical Models

The aim of this paper was to develop empirical relationships between ground cover and spectral data. Table 2 summarizes the statistics from the regression models. All of the indices chosen have significant F-ratios at 99% probability or greater. The ND6 index fits the data best, as measured by R^2 and the F test, and also has a positive intercept with the ground cover axis. Thus low ground covers can be estimated. The slope at 750 nm has the same linear shape but does not fit the data as well. The NIR/R index intersects the abcissa nearly vertically and was not useful for predicting low ground covers.

Table 3 Regression Results						
Index	X coefficient	Intercept	F-Ratio	Probability	R Squared	DF
Slope	8297	10.7	644	.00000	.90	71
ND6	135	-4.3	861	.00000	.92	71
NIR/R	-.28	.29	364	.00000	.83	71

Confidence intervals for estimation of ground cover were shown for all indices in Figures 17-19. For estimation of ground cover based on an average of six readings, the 95% confidence interval for ND6 is fairly constant at ±3% ground cover. Prediction intervals for single ground cover estimates are on the order of ±20%.

As shown in Figures 26 and 27 variation in predicted ground cover based on averages of 6 readings is much less than for individual ground cover estimates.

Spectral indices of ground cover correlate very well with ground measurements, especially field average spectral indices. The measurements were taken during varied atmospheric conditions and the data used in the correlation calculations included the different conditions.

The primary conclusion of this research is that some spectral indices of canopy development, notably ND6, can be used to determine ground cover by remote sensing.

This method of obtaining ground cover can be highly automated and can be obtained from many platforms, ranging from hand-held, post mounted, boom truck, helicopter, airplane, and satellite. (Note that the slope of the spectral curve at 750 nm, cannot be derived from currently available satellite data. The band widths of current satellite sensors are too wide to permit determination of the slope of this curve.) Spectral estimation of ground cover is also a more objective method, than the usual visual determinations.

5.2 Estimating Crop Coefficients

The motivation behind this thesis was the possibility of automating the estimation of ground cover remotely. The use of ground cover was to determine evapotranspiration crop coefficients. Traditional methods of estimating ground cover are subjective and do not adequately represent each field. Spectral estimates of ground cover may be made from many platforms.

However there is good reason to question whether ground cover is a good indicator of crop development. Other indices of crop growth might be more appropriate. Wright (1982) commented that "it would be desirable to have a means of relating crop coefficients to an index such as accumulated growing degree days or reference ET". Other indices that may be considered are biomass and leaf area. These indices may represent the plant more accurately than ground cover during closed canopy situations. Figure 30 shows the invariant nature of ground cover.

Typical methods of estimating crop coefficients involve picking the date rapid growth begins (10 percent ground cover), choosing a rapid growth line from past experience and applying that line to crop coefficient estimation (Cuenca, 1989). As Figure 29 shows, the ground cover increases rapidly after an initial 10 percent is achieved. This method assumes that each crop develops at the same rate as the crop which was used to develop the curve. The crop coefficients for potatoes developed by Wright (1982) were derived from one year of data. Due to the character of natural systems that year may not have been representative of a typical crop.

Spectral estimation of biomass and leaf area has been carried out by Jordan (1969), Pearson (1972), Asrar (1986) and others. The data taken by Chen (1991) show a relationship between LAI and NIR/R, ND6, and Slope at 750 nm. Because these indices are sensitive to plant growth throughout the season they may be a better choice for crop coefficient use than ground cover.

The variability of LAI with respect to ground cover is illustrated in Figure 3. The prediction intervals are approximately ±14.5% ground cover. The magnitude of the same intervals for ground cover versus the spectral indices is ± 18, 17, 21 percent ground cover. Different LAI have been measured at the same ground cover. Spectral reflectance depends on the amount of biomass present to reflect light.

Early season crop water use is mainly due to evaporation from the soil surface (Wright, 1982). This evaporation can be equal to ET from a reference crop (while the soil surface is wet). Thus, evaporation from the soil can be a significant part of a crop's season water use. As Chen's data indicate, remote sensing may be used to distinguish between very wet soils and dry soils to estimate soil wetness, providing the soil reflectance characteristics are known beforehand. Knowledge of qualitative soil moisture may allow better irrigation strategy. Adjustments to the crop coefficients may be made using remotely derived, soil surface moisture estimates. After ground cover has reached a detectable amount, little confidence may be had in remote soil moisture estimates. This is also the only time that surface soil moisture can be estimated well from photographic wavelength remote sensing.

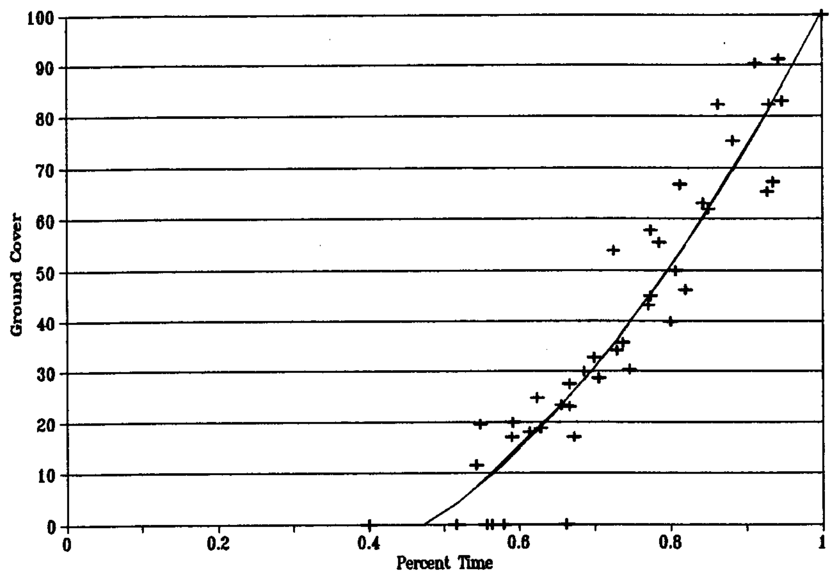

Figure 29 Ground Cover vs. Percent Time to Full Cover. Data From English (1989).

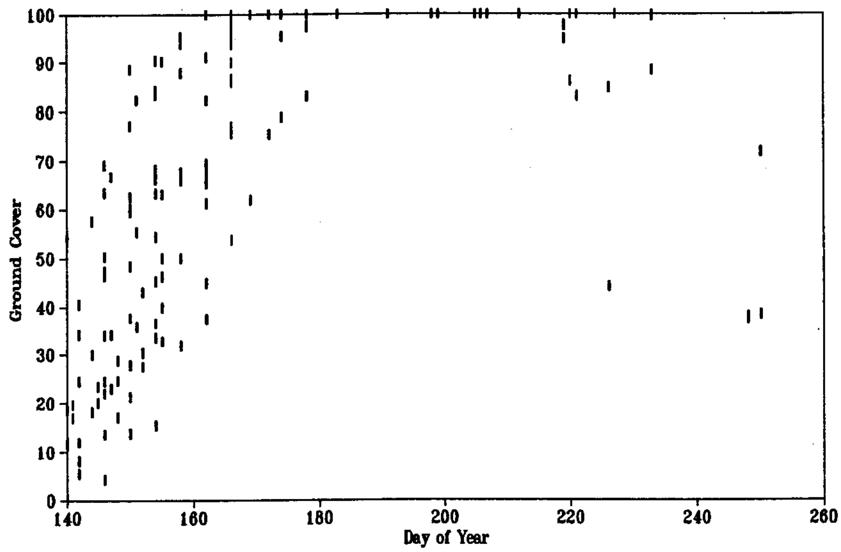

Figure 30 Ground Cover vs. Day of Year. Data From English (1989).

5.3 Recommendations

Moss (1990) has found through in-situ light interception measurements that maximum light interception for this variety of potatoes occurs at a leaf area index (LAI) of approximately 3.9. As Figure 3 illustrates, LAI varies at 100% ground cover. Indicating that ground cover may not be adequately measuring the variation present. LAI may better characterize a crop than does ground cover (GC). Crop coefficients could be based on LAI rather than GC.

LAI has been determined via remote sensing by: Asrar (1985, 1986), Jordan (1969), Tucker (1979), and Weigand (1979) as well as others. Leaf area index has been successfully estimated with several crops with near-infrared to red ratio and the normalized difference vegetation index.

Crop evapotranspiration is dependent on plant transpiration area as well as environmental conditions. The use of crop coefficients is one method to account for the transpiration area. However, crop coefficients arrive at this information indirectly through estimation of ground cover. LAI is a better index of transpiration area, and can be estimated via spectral remote sensing.

References

Asrar, G., E.T. Kanemasu, G.P. Miller, & R.L. Welsh. 1986. Light Interception and Leaf Area Estimates from Measurements of Grass Canopy Reflectance. Trans. on Geoscience and Remote Sensing. GE-24(1):76-81.

Asrar, G., E.T. Kanemasu, R.D. Jackson, P.J. Pinter Jr. 1985. Remote Sensing of Environment. 17: 211-220.

Asrar G., E.T., Kanemasu, & M. Yoshida. 1985. Estimates of Leaf Area Index from Spectral Reflectance of Wheat Under Different Cultural Practices and Solar Angle. Remote Sensing of Environment. 17:1-11.

Bauer, M.E. And C.S. Daughtry. 1986. Field Spectroscopy of Agricultural crops. Transactions on Geoscience and Remote Sensing. GE-24, No.1.

Boatwright, G.O. And V.S. Whitehead. 1985. Early Warning and Crop Condition Assessment Research. Transactions on Geoscience and Remote Sensing. GE-24:54-63.

Chen, C.F. 1991. Unpublished Ph.D. Thesis, Personal communications

Colwell, R.N. 1984. From Photographic Interpretation to Remote Sensing. Photogrammetric Engineering and Remote Sensing, (50): 1305-1307.

Daughtry, C.S.T., V.C. Vanderbilt, and V.J. Pollard. 1982. Variability of Reflectance Measurements with Sensor Altitude and Canopy Type. Agronomy Journal. (74): 744-751.

Dozier, J. And A. Strahler. 1983. Ground Investigations in Support of Remote Sensing. Manual of Remote Sensing, 2nd ed., Falls Church, Va. 959-984.

Draper, N.R., Smith, H., Applied Regression Analysis, Wiley, New York, 1966

Duggin, M.J., D.Piwinski. 1984. Recorded radiance indices for vegetation monitoring using NOAA AVHRR data; atmospheric and other effects in multitemporal data sets. Applied Optics. 23(15):2620-2623.

Duggin, M.J. and T. Cunia. 1983. Ground reflectance measurement techniques: a comparison. Applied Optics. 22(23):3771-3777.

English, M.J., Chen, C.F. 1989. Personal communications

Field, J.G. And L.G. James. 1989. Irrigation Scheduling: Plant Temperature vs Plant Reflectance. American Society of Agricultural Engineers. Paper No. 89-2028.

Gallo, K.P., C.S. Daughtry, M.E. Bauer. 1985. Spectral Estimation of Absorbed Photosynthetically Active Radiation in Corn Canopies. Remote Sensing of Environment. 17:221-232.

Gross, M.F., M.A. Hardinsky, V. Klemas. 1988. Effects of Solar Angle on Reflectance from Wetland Vegetation. Remote Sensing of Environment. 26:195-212.

Gunsaulis, F.R., M.F. Kocher, C.L. Griffis. 1989. Eliminating Surface Structure Effects on Low Organic Matter Soil Reflectance, American Society Agricultural Engineers Meeting. Paper # 89-1567.

Hatfield, J.L., G. Asrar, G. & E.T. Kanemasu. 1984. Intercepted Photosynthetically Active Radiation Estimated by Spectral Reflectance. Remote Sensing of Environment. 14:65-75.

Jackson, R. D. (1982), Canopy temperature and crop water stress, Advances in Irrigation (D. Hillel, Ed.) Academic, New York, pp 43-85

Jackson, R.D., P.J. Pinter Jr., R.J. Reginato, B.I. Sherwood. 1986. Detection and Evaluation of Plant Stresses for Crop Management Decisions. Transactions on Geoscience and Remote Sensing. GE-24(1): 99-105.

Jordan, C.F., Derivation of Leaf Area Index from Quality of Light on the Forest Floor, Ecology, 1969, 50, 663-666

Kimes, D.S. And J.A. Kirchner. 1982. Irradiance Measurement Errors Due to Assumption of a Lambertian Reference Panel. Remote Sensing of Environment. 12: 141-149.

Kimes,D.S., J.A. Kirchner, & W.W. Newcomb. 1983. Spectral radiance errors in remote sensing ground studies due to nearby objects. Applied Optics. 22(1):8-10.

Kirchner, J.A., D.S. Kimes, J.E. McMurtrey III. 1982. Variation of directional reflectance factors with structural changes of a developing alfalfa canopy. Applied Optics. 21(20):3766-3774.

Knipling, E.B. 1970. Physical and Physiological Basis for the Reflectance of Visible and Near-Infrared Radiation from Vegetation. Remote Sensing of Environment; 1: 155-159.

Kollenkark, J.C., V. C. Vanderbilt, C.S. Daughtry, & M.E. Bauer. 1982. Influence of solar illumination angle on soybean canopy reflectance. Applied Optics; 21(7):1179-1184.

Leckie, D.G., P.M. Teillet, D.P. Ostaff, and G. Fedosejevs. 1988. Sensor Band Selection for Detecting Current Defoliation Caused by the Spruce Budworm. Remote Sensing of Environment. 26:31-50.

Mestre, H., The absorption of radiation by leaves and algae, Cold Spring Harbor Symp. Quant. Biol., 1935, 3, 191-209

Millard, P., G.G. Wright, M.J. Adams, R.V. Birnie and P. Whitworth. 1990. Estimation of light interception and biomass of the potato (Solanum tuberosum L.) From reflection in the red and near-infrared spectral bands. Agricultural and Forest Meteorology. 53: 19-31.

Milton, E.J. 1987. Principles of field spectroscopy. Remote Sensing. 8(12): 1807-1827.

Moss, D.N. 1990, Personal communications

Pearson, R.L., L.D. Miller, C.J. Tucker. 1976. Hand-held spectral radiometer to estimate gramineous biomass. Applied Optics; 15(2):416-418.

Pearson, R.L., L.D. Miller, 1972 Remote Mapping of Standing Crop Biomass for Estimation of the Productivity of the Shortgrass Prairie. 8th International Symposium on Remote Sensing of Environment, 1355

Perry Jr., C.R., L.F. Lautenschlager. 1984. Functional equivalence of Spectral Vegetation Indices. Remote Sensing of Environment. 14:169-182.

Pinter, Jr. 1986. Effect of Dew on Canopy Reflectance and Temperature. Remote Sensing of Environment. 19:187-205.

Ranson, K.J., C.S.T. Daughtry, L.L. Biehl, M.E. Bauer. 1985. Sun-View Angle Effects on Reflectance Factors of Corn Canopies. Remote Sensing of Environment. 18:147-161.

Rouse, J.W. Haas,R.H. Schell, J.A. And Deering, D.W., Monitoring vegetation systems in the great plains with ERTS, Third ERTS Symposium, NASA SP351, 1973, I:309-317

Schutt, J., B.N. Holben, C.M. Shai, & J.H. Henninger.1981. Reflectivity of TFE -a washable surface-compared with that of BaSO4. Applied Optics. 20(12):2033-2035.

Shibayama, M., C.L. Wiegand. 1985. View Azimuth and Zenith, and Solar Angle Effects on Wheat Canopy Reflectance. Remote Sensing of Environment. 18:91-103.

Tappan, G. 1980, The Monitoring of Green Vegetation Cover in the Kansas Flint Hills from Landsat Data, KARS, Univ. Of Kansas, Lawrence

Tucker, C.J., J.H. Elgin, Jr., J.E. McMurtrey III. 1979. Monitoring Corn and Soybean Crop Development with Hand-held Radiometer Spectral Data. Remote Sensing of Environment. 8:237-248.

Tucker, C.J., Miller, L.D., Soil Spectra Contributions to Grass Canopy Spectral Reflectance, Photogrammetric Engineering and Remote Sensing, 1977, 43:721-726

Tucker, C.J. 1977. Asymptotic nature of grass canopy spectral reflectance. Applied Optics. 16(5):1151-1156.

Tucker, C.J. 1979. Red and Photographic Infrared Linear Combinations for Monitoring Vegetation. Remote Sensing of Environment. 8:127-150.

Weigand, C.L., A.J. Richardson, P.R. Nixon. 1986. Spectral Components analysis: A Bridge Between Spectral Observations and Agrometeorological Crop Models. Transactions on Geoscience and Remote Sensing. GE-24(1):83-89.

Wiegand, C.L., A.J. Richardson, & E.T. Kanemasu. 1979. Leaf Area Index Estimates for Wheat from LANDSAT and Their Implications for Evapotranspiration and Crop Modeling. Agronomy Journal. 71:336-341.

Wright, J.L., New Evapotranspiration Crop Coefficients, Journal of the Irrigation and Drainage Division, 1982, 108 No. IR 1.

Appendix

Appendix A
Spectral Data

					First	Normalized	
					Derivative	Difference	
	Location				@ 750 nm	Index	NIR/R
Time		JD	Field	GC	0.00430	0.387	2.263634
15.4	1	137	1	46	0.00397	0.397	2.314088
12.9	1	139	1	42	0.00433	0.418	2.43513
12.9	2	139	1	54	0.00420	0.385	2.253485
13.1	3	139	1	47	0.00526	0.447	2.615864
13.2	4	139	1	54	0.00304	0.303	1.869266
13.5	5	139	1	42	0.00380	0.351	2.082978
13.5	6	139	1	49	0.01107	0.747	6.911361
11.1	1	190	1	95	0.01107	0.740	6.681808
11.2	2	190	1	96	0.01051	0.746	6.887318
11.4	3	190	1	96	0.01091	0.739	6.670003
11.4	4	190	1	97	0.01021	0.738	6.619803
11.6	5	190	1	95	0.01127	0.739	6.651149
11.6	6	190	1	97	0.00099	0.130	1.299811
13.1	2	136	10	23	0.00155	0.164	1.392839
13.4	3	136	10	18	0.00102	0.142	1.330258
13.5	4	136	10	18	0.00159	0.177	1.431496
13.7	5	136	10	19	0.00165	0.183	1.446994
13.7	6	136	10	27	0.00268	0.352	2.086659
13.1	1	141	10	17	0.00212	0.315	1.919037
13.1	2	141	10	39	0.00294	0.362	2.1365
13.7	3	141	10	27	0.00198	0.293	1.829753
13.7	4	141	10	36	0.00301	0.384	2.249027
13.9	5	141	10	34	0.00218	0.343	2.046296
13.9	6	141	10	32	0.00912	0.682	5.280193
13.5	5	165	10	99	0.00139	0.145	1.339764
14.6	4	136	40	22	0.00086	0.137	1.318369

14.8	5	136	40	26	0.00159	0.155	1.366283
14.8	6	136	40	24	0.00096	0.132	1.305311
9.85	1	141	40	41	0.00288	0.254	1.680444
9.87	2	141	40	34	0.00251	0.238	1.625451
10.1	3	141	40	39	0.00304	0.269	1.734285
10.1	4	141	40	35	0.00261	0.232	1.603595
10.3	5	141	40	45	0.00823	0.650	4.718699
12.3	1	165	40	96	0.00952	0.675	5.161559
12.5	4	165	40	99	0.01170	0.743	6.770572
12.5	3	190	47	98	0.01243	0.735	6.545533
12.7	5	190	47	99	0.00023	0.098	1.21753
13.2	1	132	58	6	0.00066	0.160	1.381649
13.2	2	132	58	2	0.00096	0.176	1.428261
14	1	137	58	14	0.00079	0.148	1.347258
14	2	137	58	5	0.00102	0.151	1.354475
14.3	3	137	58	8	0.00050	0.135	1.312227
14.4	4	137	58	10	0.00050	0.109	1.245715
14.6	5	137	58	3	0.00056	0.115	1.261093
14.6	6	137	58	3	0.00175	0.151	1.354955
11.4	1	139	58	18	0.00116	0.130	1.298874
11.4	2	139	58	9	0.00129	0.123	1.280382
11.6	3	139	58	12	0.00073	0.122	1.276664
11.7	4	139	58	14	0.00076	0.112	1.252096
11.9	5	139	58	6	0.00066	0.115	1.260342
11.9	6	139	58	5	0.00218	0.335	2.007655
14.6	1	133	67	42	0.00258	0.353	2.093334
14.7	2	133	67	46	0.00493	0.331	1.988581
14.8	3	133	67	53	0.00383	0.313	1.909436
14.8	4	133	67	43	0.00502	0.487	2.897022
15.4	1	136	67	60	0.00446	0.488	2.903442
15.4	2	136	67	56	0.00522	0.510	3.083292
15.6	3	136	67	57	0.00486	0.509	3.073283
15.6	4	136	67	52	0.00483	0.488	2.903843

15.8	5	136	67	54	0.00430	0.456	2.673721
15.8	6	136	67	51	0.00579	0.485	2.885813
10.9	1	141	67	65	0.00579	0.485	2.887027
10.9	2	141	67	64	0.00625	0.521	3.177042
11	3	141	67	71	0.00661	0.521	3.173779
11.1	4	141	67	66	0.00641	0.471	2.778563
11.2	5	141	67	67	0.01018	0.517	3.144625
11.2	6	141	67	64	0.00671	0.708	5.84768
15.4	6	156	67	91	0.00777	0.658	4.851012
14.3	1	165	67	92	0.00883	0.710	5.887488
14.5	2	165	67	88	0.00985	0.725	6.260931
14.8	4	165	67	82	0.00896	0.718	6.101571
15	5	165	67	85			